SLAC-PUB-14149

Coherent X-ray Imaging (CXI) instrument at the Linac Coherent Light Source (LCLS)

Sébastien Boutet[1], Garth J. Williams[1]

[1] SLAC National Accelerator Laboratory, 2575 Sand Hill Road, Menlo Park, CA, 94025, USA

E-mail: sboutet@slac.stanford.edu

Abstract

The Linac Coherent Light Source (LCLS) has become the first ever operational hard X-ray Free Electron Laser in 2009. It will operate as a user facility capable of delivering unique research opportunities in multiple fields of science. The LCLS and the LCLS Ultrafast Science Instruments (LUSI) construction projects are developing instruments designed to make full use of the capabilities afforded by the LCLS beam. One such instrument is being designed to utilize the LCLS coherent beam to image with high resolution any sub-micron object. This instrument is called the Coherent X-ray Imaging (CXI) instrument. This instrument will provide a flexible optical system capable of tailoring key beam parameters for the users. A suite of shot-to-shot diagnostics will also be provided to characterize the beam on every pulse. The provided instrumentation will include multi-purpose sample environments, sample delivery and a custom detector capable of collecting 2D data at 120 Hz. In this article, the LCLS will be briefly introduced along with the technique of Coherent X-ray Diffractive Imaging (CXDI). A few examples of scientific opportunities using the CXI instrument will be described. Finally, the conceptual layout of the instrument will be presented along with a description of the key requirements for the overall system and specific devices required.

1. Introduction

In recent years, a tremendous effort has been devoted to the development of a technique called Coherent X-ray Diffractive Imaging (CXDI). In its simplest form, the technique allows an image of any isolated object to be obtained from the measurement of the diffracted x-ray intensities alone. This is achieved by using computer algorithms[1-4] to retrieve the phases associated with the intensity measurements, thereby recovering the complex amplitude of the x-ray wave at the detector. From this detector-plane wave, the exit-surface wave leaving the sample is reconstructed by simply back-propagating the retrieved complex amplitude to the sample plane. The technique relies on the ability to apply a constraint on the complex wave in both the detector- and the sample-planes and iteratively enforcing these constraints until a solution is found that matches both sets of constraints. The constraint at the detector plane is very simply that the amplitudes of the current computer iterate are replaced by the measured amplitudes, while keeping the recovered phases. A variety of constraints[3] can be used at the sample plane but typically the minimal constraint is that the sample is isolated, which forces to zero some portion of the exit-surface wave. The technique was first demonstrated on non-periodic test samples[5] and has since been extended to image crystalline samples in a Bragg geometry[6]. Recently, it was also demonstrated that having an isolated sample is not a strict requirement, as a well-characterized, finite illumination incident on an extended sample can provide a sufficiently strong constraint in the sample plane for the exit surface wave recovery[7]. Also recently,, it was shown that extended objects can be imaged by scanning the beam over the sample with sufficient overlap between the scan points[8].

Work supported in part by US Department of Energy contract DE-AC02-76SF00515.

In the majority of cases, full coherence of the x-ray beam is assumed. In practice, high quality images can be obtained with partially-coherent beams produced by third-generation synchrotron sources but a full understanding of the coherence properties of the beam is required to fully understand the results and this has been the subject of recent studies[9].

While the technique of coherent x-ray diffractive imaging has become very popular and successful, it has yet to fulfill its full potential. In theory, the image resolution should only be limited by the wavelength of the incident x-rays. In practice, some experimental limitations exist and the real resolution limit is often the extent of the detector and therefore the largest angle at which signal is measured. But this can also be limited due to the dynamic range of the detector. Coherent diffraction patterns can span many orders of magnitude in intensities and, typically, this exceeds the dynamic range of available area detectors. The effective dynamic range can be increased with multiple exposures; but, as the exposure time is increased, changes to the sample--such as motion of the sample in its illumination-- are likely to occur. These changes give rise to an incoherent superposition of diffracted intensities in the detector, which affect the reconstruction by reducing the imaging resolution and, potentially, introducing artifacts in the resulting exit-surface wave. The problem is especially severe for biological samples which, with exposure, suffer damage from the x-ray beam, changing the very structures one wishes to image. There is a fundamental limit of roughly 10 nm to the resolution one can obtain for single non-periodic biological objects utilizing conventional continuous exposures[10].

Fourth-generation light sources offer a new opportunity to circumvent the “damage problem” by allowing measurements to be performed extremely quickly, thus removing the problems associated with sample motion or radiation damage. Pushed to the ultimate, this may allow structure determination of biomolecules without the need to crystallize samples[11]. Work toward this goal has been on-going at the world’s first VUV Free Electron Laser (FEL) user facility[12], the Free electron LASer in Hamburg (FLASH)[13]. Many studies have been published demonstrating the principles involved in single shot imaging and developing the technologies required for single particle and single molecule imaging[14-17].

High resolution imaging with FELs requires new sources capable of producing x-rays in the nm and sub-nm wavelength range. These sources have recently become a reality. The first such source, the Linac Coherent Light Source (LCLS) at SLAC National Accelerator Laboratory, produced the very first FEL beam at 8 keV in April 2009. LCLS welcomed its first external users in October 2009. X-ray instruments are being designed and built to fully utilize the capabilities of the LCLS and one such instrument is primarily dedicated to performing coherent diffractive imaging experiments using single pulses of hard x-rays. This instrument is called the Coherent X-ray Imaging (CXI) instrument and this article describes its motivation, expected capabilities, and conceptual design.

2. The Linac Coherent Light Source

The Linac Coherent Light Source utilizes the last kilometer of the 3-km existing SLAC linear accelerator to accelerate electrons and pass them through up to 132 m of undulators to initiate the Self-Amplified Spontaneous Emission (SASE) process, which leads to extremely intense short pulses of coherent x-rays. LCLS commissioning is essentially complete and the machine has demonstrated the production of FEL radiation over an energy range of 800 to 9000 eV. Some machine commissioning results have been published[18-20]. The currently available beam parameters are summarized in

Table 1. In the hard x-ray regime, i.e., at 9 keV, LCLS will provide users with pulses of 80 fs or less containing $2x10^{12}$ photons per pulse. A low charge mode was also demonstrated that could allow significantly shorter pulse durations[18]. The odd harmonics of the fundamental wavelength will be present, with the third harmonic being the most intense at roughly 1% of the intensity of the fundamental.

Table 1: Summary of key LCLS parameters.

Photon Beam Parameters	**Symbol**	**Hard x-rays**	**Soft x-rays**	**Unit**
Fundamental wavelength	λ_r	≥1.4	≤17	Å
Photon energy	$\hbar\omega$	9000	750-2000	eV
Final linac e^- energy	γmc^2	14.2	4.1	GeV
FEL 3-D gain length	L_G	3.3	1.5	m
Photons per pulse	N_γ	2	20	10^{12}
Peak brightness	B_{pk}	20	0.3	10^{32} [a]
Average brightness (30 Hz*)	$\langle B \rangle$	40	2	10^{20} [a]
Photon bandwidth	$\Delta\omega/\omega$	~0.2	~0.4	%
Bunch charge	Q	0.25	0.25	nC
Final pulse duration (fwhm)	$\Delta\tau_f$	80	240	fs
Electron Beam Parameters				
Single bunch rep. rate	f	30[b]	30[b]	Hz
e^- energy stability (rms)	$\Delta E/E$	0.04	0.07	%
e^- x,y stability (rms)	x/σ_x	15, 10	25, 20	%
e^- timing stability (rms)	Δt	50	N/A	fs
Peak current stab. (rms)	$\Delta I/I$	10	6	%
Charge stability (rms)	$\Delta Q/Q$	2.5	2.5	%
FEL pulse energy stability	$\Delta N/N$	<10	<10	%

[a] Repetition rate is expected to be increased to 120 Hz in 2010.

[b] Brightness units are photons/sec/mm^2/mrad^2/0.1%-BW.

Extensive machine development and research efforts are ongoing at LCLS to expand the operational parameters. While some of these improvements are only conceptual at this point, it is conceivable that in the near future LCLS could offer much expanded capabilities with an increased photon energy range both at the short- and long- wavelengths, as well as chirping capabilities and the ability to control the pulse duration over a wide range of values. All these improvements, should they become a reality, are expected to greatly benefit all scientific programs at LCLS.

2.1. LCLS front-end optics

In addition to producing SASE radiation under the right beam conditions, the electron beam passing through the long undulator also produces spontaneous radiation. This spontaneous radiation comes as pulses of roughly the same duration and at the same rate as the FEL radiation. The total spontaneous power generated is one order-of-magnitude larger than the FEL power. The spectrum of the spontaneous background extends to very high energies as it does for a typical hard x-ray undulator at a third generation synchrotron source.

It is necessary to remove this spontaneous background from the beam upstream of the experimental stations. The spontaneous source is incoherent and diverges much faster than the

FEL beam. This allows a simple way to remove it. Located roughly 100 m from the exit of the undulator are offset mirror systems which reflect the FEL beam and spatially filter the spontaneous background. These mirrors are highly polished grazing incidence mirrors. The grazing angle sets at high energy cutoff above which the x-rays are not reflected and therefore the mirrors also act as bandpass filters.

The LCLS Front End Enclosure includes two sets of offset mirrors, creating two distinct x-ray branches as shown on Figure 1. The soft x-ray branch includes mirrors M1S, M2S, M3S1 and M3S2 and has a high-energy cutoff of 2 keV while the hard x-ray branch, with mirrors M1H and M2H has a high energy cutoff of 25 keV. This allows the LCLS third harmonic to be used up to an energy of 25 keV. The offset mirror systems and their simulated impact on the beam profile has been discussed previously[21]. The CXI instrument will be installed on the hard x-ray branch of LCLS, in Hutch 5 in the Far Experimental Hall (FEH). The CXI hutch is located 383 meters away from the exit of the undulators. In theory, CXI should be capable of using any energy x-ray produced by LCLS, up to the 25 keV limit imposed by the offset mirrors. However, the LCLS beam diverges rapidly at low energies and due to the small incidence angle required to reflect the 25 keV beam, the hard x-ray offset mirrors have a very small clear aperture (500 μm) relative to the beam size below 2 keV. Therefore, the CXI instrument will operate only in the 2-25 keV range. In the 2-4 keV range, it is expected that some diffraction effects will impact the beam quality due to the limited aperture of the hard x-ray offset mirrors, as shown on Figure 2.

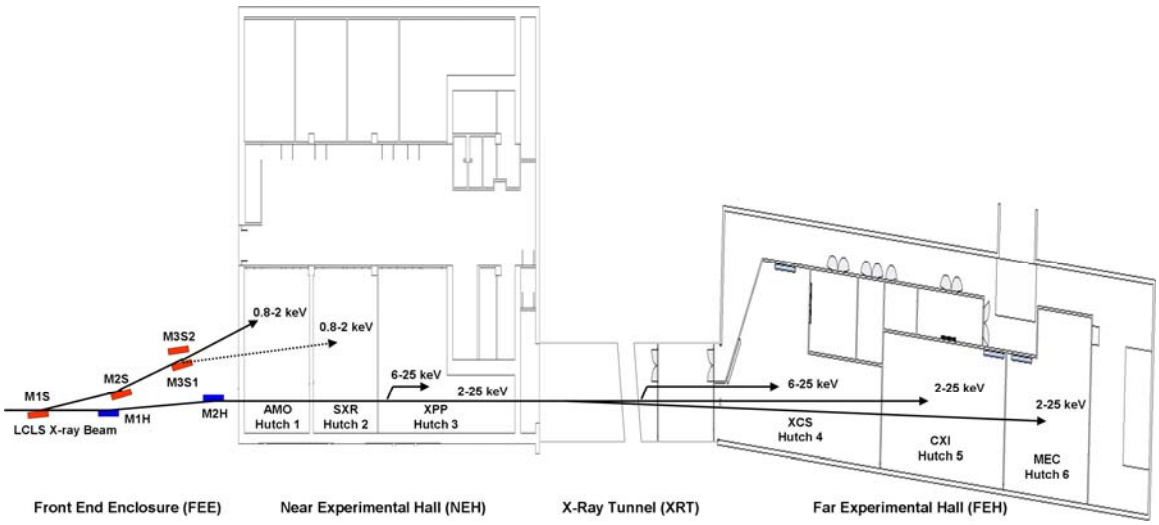

Figure 1: Layout of the LCLS Front End Enclosure and experimental halls. The soft x-ray branch is served by the soft x-ray offset mirror system (in red) and the hard x-ray instruments are served by the hard x-ray offset mirror system (in blue). The CXI instrument will be located on the hard x-ray branch in Hutch 5 of the Far Experimental Hall. Other LCLS instruments are the Atomic, Molecular and Optical science instrument (AMO) in Hutch 1, Soft X-Ray materials science (SXR) in Hutch 2, X-ray Pump-Probe (XPP) in Hutch 3, X-ray Correlation Spectroscopy (XCS) in Hutch 4 and Matter in Extreme Conditions (MEC) in Hutch 6. The energy range at which these instruments will operate is shown in each hutch on the figure. Figure not to scale.

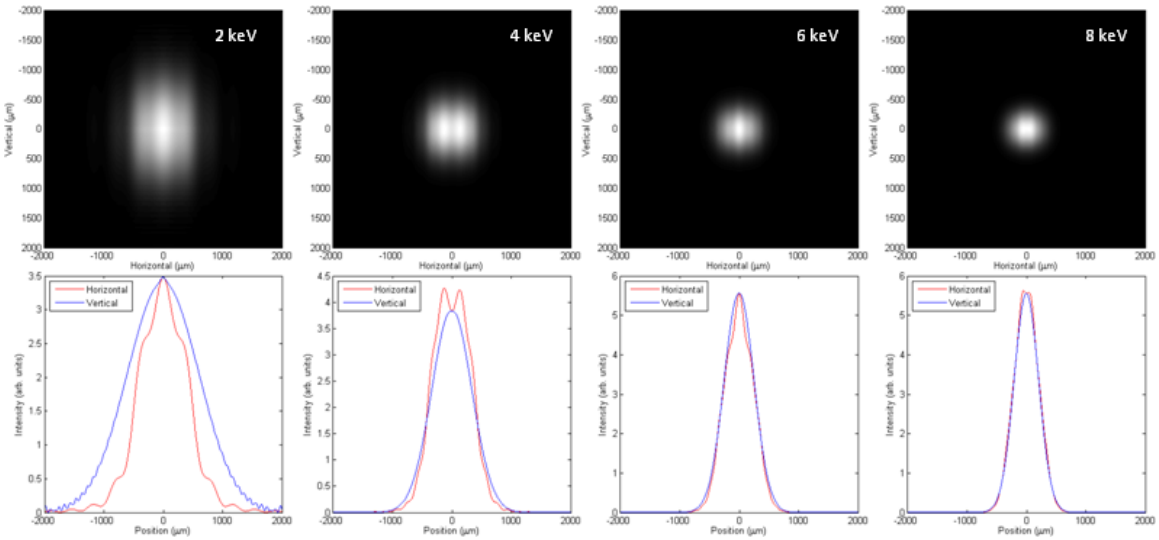

Figure 2: Calculated beam profiles at the CXI instrument for various photon energies calculated assuming a Gaussian source. The top row shows the 2D profiles while the bottom row shows the horizontal and vertical 1D profiles through the center of the beam. The finite aperture of the LCLS hard x-ray offset mirrors causes significant diffraction effects at energies below 4 keV. Perfect optics are assumed for these calculations and wavefront distortions from the mirror height-errors is neglected.

3. Coherent diffractive imaging technique

The technique of coherent diffractive imaging is conceptually very simple and comes in a few different flavors, as discussed in the introduction. In the simplest form, it only requires a coherent beam illuminating an isolated sample and a 2D detector located in the far-field to measure the diffracted intensities from the isolated sample. A beamstop is typically required to absorb the intense direct beam and protect the detector. In the case of FEL imaging, as will be the case at LCLS, a beamstop cannot be used since it would suffer ablation by the direct beam and eventually fail. The ablation process would lead to plasma formation, which would glow and cause an unacceptable background on the detector. Therefore, special detectors, which have a central hole to let the direct beam safely pass through, need to be used.
In most cases, some focusing optic is used to closely match the extent of the beam to the sample size and maximize the signal level. The focal spot size and the sample-to-detector distance must be adjusted for a given sample and any instrument designed to use the technique must have the flexibility to adjust these parameters.

The coherent diffractive imaging technique, as implemented in the CXI instrument, is a forward-scattering technique in which the diffraction pattern is measured as it expands in a cone in the forward direction. The CXI instrument is therefore designed to measure forward scattering from any sample. Small Angle X-ray Scattering (SAXS) and Wide Angle X-ray Scattering (WAXS) patterns can be measured using CXI. SAXS and WAXS differ from coherent diffractive imaging only in the coherence of the illumination, the isolated nature of the sample and the method in which the data is analyzed, so these experimental geometries are well-suited to the instrument. The CXI instrument is compatible with many x-ray scattering and diffraction techniques and a few examples of the potential scientific applications are given in the next section.

4. Coherent X-ray Imaging instrument scientific program

4.1. 2D imaging of irreproducible samples beyond the damage limit

It was suggested in 2000 that a sufficiently short and intense pulse of hard x-ray radiation could be used to overcome the fundamental radiation damage problem associated with imaging single, non-periodic biological structures[11]. During any time-integrated illumination of a radiation-sensitive sample such as any biological object, the x-rays used to probe the structure cause this same structure to be modified due to the interactions with the sample. The number of x-rays needed to resolve objects below roughly 10 nm exceeds the number of x-rays required to destroy the features of interest. This is a fundamental limit which cannot be surpassed for any measurement performed over time scales longer than the damage processes, as is always the case at synchrotron facilities. The CXI instrument at LCLS will allow this radiation damage limit to be overcome by performing the measurements in a few tens of femtoseconds or less using 10^{12} photons or more per pulse. Imaging of the samples will be done using single shots in which the sample is completely destroyed by the beam only after the structure-encoding 2D diffraction pattern has been recorded. Using this technique, each sample can only be studied for one pulse since it has been destroyed long before a second pulse arrives.

For irreproducible objects such as biological cells or any unique sub-micron particle, the information which can be obtained from a single shot measurement is limited to 2 dimensions, although schemes have been proposed to obtain 3D information from one FEL pulse[22]. Any image of an irreproducible object in 2D obtained using a single LCLS pulse will represent the projection of the entire object onto a plane parallel to the 2D detector. This will certainly complicate the interpretation of the resulting image by blurring the features of the sample. This reduces the contrast but does affect the resolution of the image. It does make it more difficult to distinguish features, especially for thicker objects where more features from different planes are projected onto the image plane. In cases where lots of different internal features exist, it is more likely that the projection image will average out to a uniform density which would make it impossible to discern any of the internal structure. However, in some cases where a few distinct internal features are present in an otherwise uniform sample, it would be possible to obtain high resolution structural information about specific features, albeit with some contamination from the projection. One possible example would be the nucleus inside an otherwise fairly homogenous cell.

In the case of biological cells, LCLS offers unique possibilities to obtain 2D images beyond the damage limit of fully hydrated living cells, a possibility which no other technique can offer. The CXI instrument will implement new sample delivery techniques which allow free-standing samples to be transferred to the high vacuum of the sample chamber rapidly and if necessary, deliver the samples in a hydrated state. This will allow living cells to be imaged as they fly through the interaction region with the LCLS beam. The CXI instrument will be fully compatible with sample delivery techniques developed at FLASH and the Advanced Light Source[16, 17, 23-25].

4.2. Single Molecule Imaging

The coherent diffractive imaging technique was demonstrated in three dimensions using a rotation stage to tomographically illuminate a sample over a range of orientations and record 2D diffraction patterns at multiple angles. Each 2D diffraction pattern represents a slice in the 3D reciprocal space and, when properly assembled in a 3D array, they can be used to obtain a 3D image of the object[26]. Such tomographic measurements are possible using the CXI instrument

but would require attenuation of the LCLS beam to the level where the sample can survive multiple shots, bringing the intensity of the incident beam in the range of third generation synchrotron sources which would negate the uniqueness of the FEL beam.

Three-dimensional imaging is possible at LCLS using single shot diffract-then-destroy measurements of identical objects in different orientations. Samples can be delivered to the LCLS beam in a particle beam with random orientation and if sufficiently many identical objects are illuminated and 2D diffraction patterns are recorded, all the data necessary to obtain the 3D image of the object is in theory available. The technical challenge comes from the difficulty of detecting very low signals from the small samples and the fundamental question of how truly reproducible samples can really be. Also the random and unknown orientation of each 2D diffraction pattern makes it extremely challenging to analysze the data. The relative orientation of each pattern must be recovered from the diffracted intensities alone without any prior knowledge. Multiple computer algorithms have been proposed over the years [27-31] and offer promising possibilities of success even given large amount of noise in the experimental data.

Should it be proven possible to assemble the three-dimensional data set from randomly oriented copies of the same object, the CXI instrument will allow biological macromolecules which cannot be crystallized to be imaged at a resolution limited only be the wavelength of the X-rays, the size of the detector, the true reproducibility of the samples, the scattering strength and the structural damage during the pulse. Macromolecular crystallography is today the primary technique for solving the atomic structure of biomolecules and the technique has been extremely successful, once large, high-quality crystals are produced. Unfortunately, for many biomolecules, crystallization can either take years or simply fail; the CXI instrument hopes to provide a complementary technique to solve the structure of biomolecules that are not amenable to traditional x-ray structure determination techniques. For example, membrane proteins are famously difficult to crystallize and also extremely important to metabolic processes. Yet very little is understood about their structure and the CXI instrument could have a large impact by providing a new method to study these molecules.

4.3. Protein nanocrystallography

While growing large, high-quality macromolecular crystals suitable for structure determination is often challenging, in some cases it is possible to produce a large number of crystals that are too small to be used at a synchrotron facilities. If a large number of such crystals--which can be sub-micron in size--can be produced, then the CXI instrument offers a way to solve the macromolecular structure in a way similar to single molecule imaging described above. A series of nanocrystals can be illuminated one-by-one, each by a single LCLS pulse which destroys them but not before a diffraction pattern is recorded. Contrary to the case of a single molecule, where the diffraction pattern is a weak continuous function, the periodic structure of the nanocrystals gives rise to intense Bragg peaks which can be indexed using standard methods. Each exposure of a single nanocrystal will excite a large quantity of Bragg reflections due to the large natural bandwidth of the LCLS beam (~0.2%). The Bragg peaks greatly facilitate the determination of the relative orientation of each nanocrystal, assuming they all possess the same crystal structure, due to the expected high signal-to-noise ratio at high resolution compared to single molecules.

New data analysis tools will be required for such measurements in order to deal with the partial Bragg reflections which will occur since the sample is not rotated to capture the full intensity of the Bragg peaks. It should be possible to appropriately account for that by averaging many diffraction patterns from similar orientations.

Protein nanocrystallography using the CXI instrument at LCLS will offer new possibilities to determine the structure of a whole new set of molecules which could not be studied before due to the lack of large high-quality crystals. It is less challenging experimentally and computationally than single-molecule imaging and offers an intermediate step between crystallography with large crystals and single-molecule imaging.

4.4. Other coherent imaging techniques

A host of different imaging techniques which utilize the coherence properties of an X-ray beam have been demonstrated. Among those are holographic techniques including Fourier Transform Holography[32, 33], multiple reference as well as extended reference holography[15, 34, 35] and massively parallel holography[36], which require a sample to be prepared next to a reference object of some kind. All of these techniques can be exploited using the CXI instrument with a suitably prepared sample on a fixed mount. It may also be possible to prepare or deliver free-standing samples that include a reference object. The key advantage of all these holographic techniques is the relative simplicity of obtaining the orientation of the sample through a simple mathematical transform. These techniques could simplify the process of determining the relative orientation of identical objects illuminated by the beam. Also, some of these techniques can be used to enhance the signal from weakly scattering objects by interfering the diffracted wave from the weak object with the wave from a strong reference. This could allow much smaller objects to be imaged using the LCLS beam[15, 35].

Other coherent diffractive imaging techniques, e.g., include Fresnel Coherent Diffractive Imaging[37],Ptychography[8], etc., can also be implemented at the CXI instrument but pose important technical challenges. For example, the Fresnel CXDI experiments require very accurate knowledge of the illumination of the sample. In order to use this technique for single-shot imaging, one would need a technique to determine the wavefront of every LCLS pulse since the random nature of the FEL process leads to fluctuations in the wavefront. Also, the source size and location fluctuate shot-to-shot which modifies the curvature of the wave at the sample. With a proper single-shot wavefront diagnostic and the means to accurately determine the sample position relative to the focus, Fresnel CXDI does offer great advantages compared to plane-wave CDI due to the better convergence of the algorithms and the uniqueness of the solution. However, another key technical challenge for single-shot Fresnel CXDI is the larger dynamic range required for the detector, which is very challenging for single-shot measurements.

As for Ptychography, the technique requires overlapping illuminations of a large sample which requires the sample to survive multiple exposures. Once the beam is attenuated enough for the sample to survive multiple exposures, the advantages of LCLS compared to a synchrotron source are less obvious.

Another branch of the coherent diffractive imaging applications involves the study of crystal shapes and strain in the Bragg geometry[6]. Such experiments will not be feasible using the currently envisioned CXI instrument but other instruments at LCLS, such as the X-ray Correlation Spectroscopy (XCS) and X-ray Pump-Probe (XPP) instruments, will make these measurements possible.

4.5. Nanoprobe

The initially planned focusing optics for the CXI instrument will include the capability to produce a 100 nm focus. Other optics could potentially be used to produce a smaller beam down to a few tens of nm or less[38]. Even with a 100 nm focus, there are opportunities to use the CXI instrument as a nanoprobe to study the local structure of a sample. The detector used in the CXI instrument will have the capability to read the data at 120 Hz, the repetition rate of the LCLS and therefore allows the possibility of mapping with single shots a very large area on a sample in a manageable amount of time.

The diffract-then-destroy imaging technique could be used for such measurements; however, since the damaged area on the sample will extend slightly beyond the size of the beam itself, a scan on the sample would not represent a continuous region with successive scan points required to be far enough apart to stay away from the previous damage. The CXI sample chamber is sufficiently flexible to allow for additional detectors, e.g., to collect fluorescence, which could provide information complementary to the imaging detector.

4.6. Nucleation studies

The process of crystal nucleation is not fully understood and represents a very important problem, especially as it relates to macromolecular crystal formation. Attempts have been made using synchrotron radiation to study the formation of sub-micron protein crystals in-situ in order to study their structure at different stages of the crystal nucleation and growth process[39-41]. There are many challenges to doing this using a synchrotron beam that can be alleviated by using the LCLS beam in the CXI instrument. For example, instantaneous snapshots can be taken, removing errors due to a nanocrystal moving in solution during the measurement. Single LCLS pulses can provide enough intensity for a full 2D measurement without the need to use multiple exposures, which ameliorates radiation damage issues in analogy to the diffract-then-destroy concept.

A supersaturated solution could be flowed through the LCLS beam and the 2D detector would be set some distance away from the sample which allows the powder ring of the low order Bragg peaks to be measured. Samples could also be delivered using the particle injection techniques developed at FLASH and the ALS[16, 23, 24].Then, as crystals form from solution or move into the beam, single Bragg peaks would appear on the detector and these would show interference fringes representative of the crystal shape and internal strain. It would be possible to collect data at 120 Hz and wait for random occurrences when a small nanocrystal forms with the proper orientation in the beam. It might be possible to study the formation of critical nuclei this way and also study the early stages of the crystal growth phase. The signal from a single nanocrystal scales as $N_{cryst}^2=L^6\rho_c^2$ where N_{cryst} is the number of unit cells in the crystal, L is the size of the crystal and ρ_c is the number density in the crystal. There will be a background signal from the solution scattering that will scale as the total number of particles within the focal volume in solution. The focal volume is given by $V_{foc}=2\pi\omega_0^2L_R=2\pi^2\omega_0^4/\lambda$ where ω_0 is the waist of the focused beam (FWHM/2.35), L_R is the Rayleigh length of the focused beam and λ is the wavelength. The total number of particles within this volume is given by $\rho_{sol}V_{foc}$ where ρ_{sol} is the number density of the solution. The signal to background ratio will then be given by $N_{cryst}^2/N_{sol}= L^6\rho_c^2\lambda/2\pi^2\rho_{sol}\omega_0^4$. For the CXI instrument, foci of 100 nm and 1μm FWHM will be possible. If one assumes that the crystal density is 100 times larger than the solution density, then the signal from the nanocrystal would be of the same strength as the solution background for a 9 nm crystal using the 100 nm FWHM focus and for a 45 nm crystal using the 1 μm FWHM focus. The solution scattering background will be fairly uniform despite the coherent illumination and could be subtracted out,raising the possibility that crystals approaching these sizes could be imaged. The situation

could be made even better by using a sample delivery technique that produces the sample inside a small droplet, which reduces the background even further.

For such experiments, the goal would be to measure the shape and strain of nanocrystals, which requires accurately sampling the diffraction pattern around a single Bragg peak as demonstrated in [6]. Crystals in the Bragg condition will generate Bragg peaks on a ring on the detector. To measure a single Bragg peak, the number of nanocrystals oriented in the Bragg condition illuminated by a single pulse of LCLS needs to be kept low to prevent multiple Bragg peaks from different crystals from overlapping on this ring. It would be relatively easy to prepare a sample with the proper density to make the probability of overlapping Bragg peaks very low. In any case, it would be easy to distinguish a single Bragg peak from a case where 2 Bragg peaks from different crystals overlap. Such a pattern would likely not display centrosymmetry and could be rejected by simple visual inspection.

A more complicated situation arises due to the fact that only a single 2D view of the nanocrystal can be obtained. There is no guarantee that the Bragg peak measured corresponds to the perfect Bragg condition. Such a misalignment would mean that the 2D slice through the Bragg peak does not go exactly through the center of the peak and would lead to a non-centrosymmetric diffraction pattern which would be difficult to distinguish from a strained crystal, which would also display a lack of centrosymmetry. In practice however, visual inspection of the diffraction patterns would allow one to determine if the center of the Bragg peak was measured since an oriented, strained crystal would produce a diffraction pattern with significantly higher symmetry than that of a misoriented crystal.

4.7. Pump-probe imaging studies

In its initial phase, the CXI instrument will not provide a pump laser system. This is, however, expected to be added in the near future since one of the most interesting aspects of the LCLS beam is the short pulse duration, which can allow exquisite time resolution for the study of dynamic processes. A sample can be prepared or pumped into a controlled state and the time evolution following this pump can be measured with 100 fs resolution or possibly better. In order to obtain this time resolution, the duration of the pump must be short and known to this level of accuracy. Typically, this requires a femtosecond laser pump pulse to excite the sample.

A wide variety of experiments can be envisioned using time-resolved imaging. The feasibility of such measurements was demonstrated at FLASH[42]. One can imagine studying destructive processes in which a powerful laser is used to ablate or shock a sample and the X-ray beam from LCLS is used to image the structure at later time. One can also use a gentler laser pump to induce reversible changes in a sample--which is then probed, either destructively or non-destructively, by the LCLS beam. For example, recent studies demonstrated laser-induced nucleation[43] which could be studied using the CXI instrument with high spatial and temporal resolution.

4.8. Nanomaterials

While the CXI instrument was originally conceived to perform measurements using biological samples and ultimately single molecules, it is in no way restricted to the use of biological samples. The hardware that will be available can be used to deliver any sample in the size range of roughly 1 μm or less to the LCLS beam to be imaged. The CXI instrument provides an unmatched capability to study the morphology of free-standing aerosols, which have impact on environmental and medical sciences[17], and offers unique opportunities in the imaging of

nanomaterials. While many areas of materials science are best addressed at the mesoscale--where the CXI instrument can provide nanometer-scale images of micron-sized objects--there exists an interesting subset of problems that depend explicitly upon the nanoscale and whose behavior can be dominated by surface, rather than bulk, effects. One previously identified example of this is semiconductor quantum dots[44], where models of an individual dot use its physical properties, e.g., size and shape, to explain behavior. Another interesting system to consider is nanocatalysis[45], where an in situ experiment at a source like the LCLS could reveal not only the size, shape, and strain distribution within a single crystalline domain of the catalyst material, but also the time evolution of these properties. Such an experiment would combine the traditional strengths of x-ray imaging in examining complicated systems with the unique peak brightness of the LCLS, which enables the coherent imaging, and its inherently pulsed nature.

5. Requirements and conceptual design of the CXI instrument

5.1. CXI hutch

The CXI instrument will be located in Hutch 5 of the Far Experimental Hall (FEH) at LCLS. The FEH is shown in Figure 3. The CXI hutch dimensions are 20 x 8 m^2 which allows sufficient space for the instrumentation described below. The dimensions of the hutch may appear large compared to the standard hutches at third-generation synchrotron sources. However, beamlines at these facilities often have multiple hutches for optics and front-end devices with a devoted experimental hutch. In the case of LCLS, each instrument occupies a single x-ray beamline with serial operation among the instruments. This means that all CXI-specific devices cannot be installed anywhere but in the experimental hutch, occupying much of the available space.

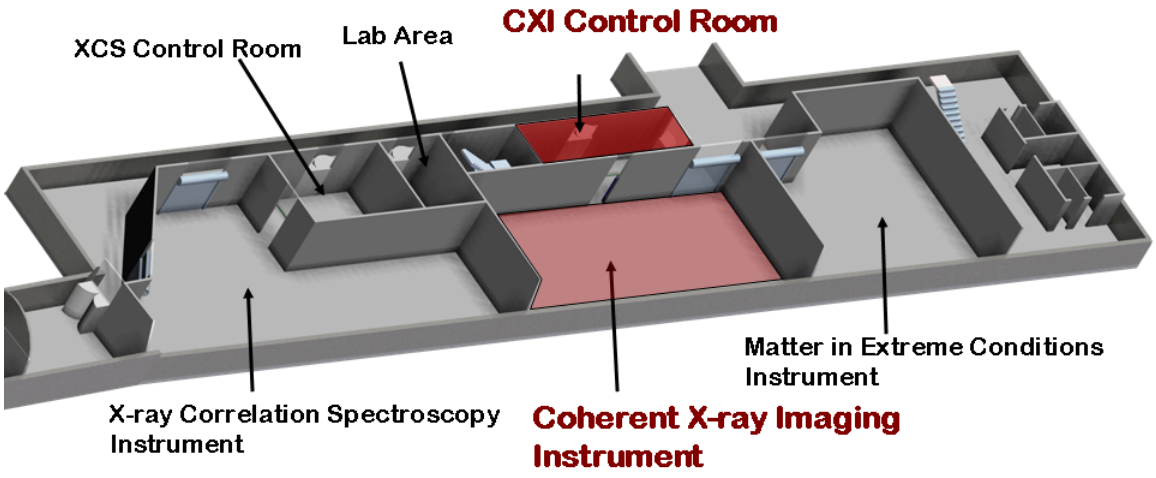

Figure 3: Architectural view of the Far Experimental Hall at LCLS showing the CXI instrument location and its control room. The CXI instrument is located in Hutch 5, which is 20 m long by 8 m wide.

5.2. CXI instrument goals

The main goal of the CXI instrument is to allow users to measure the coherent diffraction pattern from any sub-micron object using single LCLS pulses. In typical operation, these patterns will be used to form an image of a given sample at the highest possible resolution. In the case where the sample is not reproducible, the instrument will allow 2D images to be obtained while, for reproducible objects, it may be possible to obtain a full 3D image. A second goal of the CXI instrument is to allow imaging of biological samples beyond the classical radiation-damage limit

using single, ultrafast LCLS pulses. This will be achieved using the diffract-then-destroy technique pioneered at FLASH. Finally, a third goal of the CXI instrument is to deliver a reliable and flexible beam to users that allows a wide range of experiments to be performed, such as those described briefly in the previous section.

5.3. CXI global requirements

The achievable resolution for single shot imaging at the CXI instrument will be determined by a host of parameters such as the scattering strength of the sample, the size of the sample, the dynamic range of the detector, the size of the detector, the X-ray wavelength, the knowledge of the incident wavefront, the reproducibility of the sample and the damage during the pulse. How all these parameters conspire to affect the resolution of the image is very complicated and the topic of intense research. It is important that the CXI instrument be flexible and versatile, allowing parameters to be optimized for a given sample or experiment. Therefore the first key, global requirement of the instrument is to tailor the X-ray beam parameters to match the needs of the users. The beam parameters which can be controlled at CXI are the spatial profile, the intensity, the repetition rate, the wavelength and the pulse duration. These are either controlled by local optical elements at CXI or by the LCLS electron beam parameters.

The nature of the SASE process which creates the LCLS beam leads to unavoidable fluctuations of the key beam parameters on a shot-to-shot basis. In order to properly perform an experiment using the LCLS, these parameters must be characterized to the extent possible for every shot. CXI is provides a suite of diagnostics to characterize the beam parameters. These diagnostics will be discussed in more detail below.

Another key requirement of the CXI instrument is to provide a suitable sample environment to allow single-shot imaging experiments. The sample environment in most cases requires a high vacuum and the sample can either be held on a fixed target or delivered to the LCLS beam in a free-standing manner. The CXI instrument will provide the necessary equipment for the sample to be brought to the beam in vacuum either supported or free-standing.

Finally, the CXI instrument aims to perform coherent diffractive imaging experiments, which require that the high-quality wavefront of the LCLS source is preserved to the fullest extent possible. All CXI optical elements have been designed to minimize their impact on the wavefront quality.

5.4. CXI devices and associated requirements

5.4.1. Slits .In order to fully utilize the LCLS capabilities during single-shot measurements, the CXI instrument must use every photon from the FEL beam to maximize the detected signal from weakly scattering, small samples. The LCLS beam has a roughly Gaussian profile surrounded by a halo of spontaneous radiation and noise coming from beamline components. This halo must be removed without affecting the FEL beam and this will be achieved using slits made of four independently moving blades. The requirements for the slit blades are:

- limited scattering which is achieved using highly polished cylindrical blades[46],
- 10^{-8} or less transmission over the entire energy range of 2 to 25 keV,
- < 2 μm positioning accuracy and repeatability,
- 0-10 mm gap setting range,
- 10 mm-center-position setting range, and

- able to withstand the full unfocused LCLS flux.

In order to build the most efficient slit, the heaviest and therefore most X-ray absorbing material which does not get damaged by the beam must be identified and selected. Calculations of damage thresholds of materials yielded silicon nitride as the most suitable material for the slit blades capable of stopping the fundamental hard X-ray beam of LCLS. A heavier material is needed to stop the third harmonic, which will reach up to 25 keV, but the reduced intensity of the third harmonic compared to the fundamental allows heavier materials to be used without damage.

5.4.2. Attenuators. The purpose of the attenuators is to reduce the intensity of the beam and also to control the ratio of the fundamental to the third harmonic component of the LCLS beam. The key requirements are:

- 10^8 attenuation at 8.3 keV,
- 10^4 attenuation at 24.9 keV,
- 3 steps per decade for > 6 keV,
- minimize wavefront distortions, and
- able to withstand the full unfocused LCLS flux without damage.

These requirements are best fulfilled with a set of 10 filters each of varying thickness that can be inserted independently. The filters were chosen to be made of silicon since this material provides some of the best available optical quality, which is desirable in order to minimize the distortions of the wavefront, and is expected to survive the full power of the LCLS beam at the CXI location.

5.4.3. Pulse Picker. This device is required to select single pulses of the LCLS for fixed target experiments while allowing the electron beam to operate at a higher rate for better stability. It allows a single pulse to interact with the sample when desired and protects the sample from unwanted damage. The pulse picker can also be used to select a certain pattern of pulses or reduce the repetition rate of the beam at the experiment. The requirements are:

- < 3 ms switching time,
- < 8 ms in close/open cycle time, and
- able to withstand the full unfocused LCLS flux without damage.

The pulse picker is designed only to operate at 10 Hz or less. For operation above 10 Hz, the electron beam can be used to set the repetition rate at the experiment.

5.4.4. Intensity monitor. The main purpose of the intensity monitor is to provide an intensity measurement at multiple points along the beamline in order to facilitate the alignment of key optical components. The requirements are:

- remotely retractable,
- relative accuracy < 1%,
- working dynamic range of 100,
- large sensor area 20x20 mm^2, and
- single pulse operation (120 Hz).

The intensity monitor will consist of a photodiode and will therefore be a beam-destructive device that will be inserted upstream of the interaction region during the alignment of optics.

5.4.5. Profile monitor. The profile monitor also serves the purpose of aiding in the alignment of X-ray optics by providing a characterization of the X-ray beam spatial profile. It will also serve the purpose of allowing a characterization of the effects of the optics on the quality of the

coherent LCLS beam. Also, the profile monitor will provide a characterization of the X-ray beam spatial jitter and provide a beam position feedback measurement. It should:

- be remotely retractable,
- possess 12x12 mm^2 field of view with 50 μm resolution,
- possess 1x1 mm^2 field of view with 4 μm resolution, and
- be capable of single pulse operation (120 Hz) if required.

The profile monitor will consist of a scintillator screen normal to the LCLS beam and a mirror at 45 degrees to look at the scintillation signal with a camera. The screen will be destructive of the beam; therefore,the profile monitor will be inserted upstream of the interaction region during the alignment of key optical elements and retracted during measurements.

5.4.6. Intensity-position monitor. The purpose of the intensity-position monitor is to provide a non-destructive pulse-by-pulse measurement of the intensity for normalization of the data. The requirements for this device are:

- retractable (if necessary),
- highly transmissive (> 95%),
- relative accuracy of < 0.1%,
- working dynamic range of 1000,
- position accuracy of < 10 μm,
- single pulse operation (120 Hz), and
- able to withstand the full unfocused LCLS flux without damage.

The intensity-position monitor will consist of a transmissive thin foil with four downstream-facing diodes, one in each quadrant with a central hole. The beam will pass through the hole in the diodes, then through the thin foil. The Compton backscattering from the foil will be measured by the diodes providing an intensity measurement. The use of four diodes has the added benefit of providing a rough measurement of the position of the beam on each pulse, from the ratio of the measured intensities on each diode.

5.4.7. Wavefront monitor. The wavefront monitor is the name given to a device that will be, in its initial implementation, similar to the profile monitor. It will consist of a scintillator screen and a camera installed in the same way along with an extra provision for mounting an attenuator in front of the scintillator, which will prevent saturation or damage. The wavefront monitor will allow the direct beam intensity to be measured as well as the low-angle, diffracted signal that passes through the hole in the main detector. Since the phases of the beam will not be measured, phase retrieval techniques would have to be used to recover the wavefront at the focus although some technical challenges make this uncertain. For example, it is unclear at this time if a sufficiently strong constraint can be applied at the exit of the focusing optics to enable a reliable reconstructed wavefront. The reason for this is that the focusing optics were specified with a large clear aperture so as to not significantly aperture the beam. As a consequence, no strong constraint or support exists at the focusing optics. At a minimum, the wavefront monitor will provide low-angle data by acting as a second detector and will also provide a beam position feedback to the focusing optics.

5.4.8. Reference laser. The purpose of the reference laser is to provide a visible reference beam which is collinear with the LCLS beam and can be used to obtain a rough alignment of the system. The reference laser system also allows maximizing the use of beam time by providing the ability to align the experiments without using the LCLS beam. The requirements are:

- on/off states;

- smallest possible beam size throughout the hutch;
- low divergence;
- long term stability;
- useable with any part of the instrument vented to air, which requires window valves everywhere downstream of the laser;
- aligned to the unfocused FEL beam to within 100 microns.

The reference laser beam will be introduced into vacuum at the entrance of the CXI hutch and will provide a reference for all possible CXI focusing configurations.

5.4.9. X-ray focusing lenses. The CXI instrument will provide the ability to tailor the focal spot size to the sample size. This will be achieved using three main focusing optical elements to produce a 10 μm, a 1 μm and a 100 nm FWHM beam. Given the LCLS source size and the location of the CXI instrument, a 60 m focal length is required in order to produce a 10 μm focus and therefore an in-line focusing system is required. Beryllium compound refractive lenses[47] were selected because they meet the requirements of in-line focusing and can withstand the full LCLS beam without damage. Three stacks of lenses will be used in order to provide focusing at multiple photon energies since these lenses are chromatic.

5.4.10. 1 micron KB mirrors. In order to produce the 1 μm and the 100 nm foci, much shorter focal lengths are required which allows focusing mirrors to be used in a Kirkpatrick-Baez (KB) geometry. The key requirements of the 1 micron KB mirrors are:

- 8.5 m average focal length,
- large aperture to accept 4 sigmas or more of the LCLS beam,
- able to withstand the full unfocused LCLS flux without damage,
- satisfy the Marechal criterion which limits the wavefront distortions to $\lambda/14$,
- reflective over at least 2-10 keV range,
- high pointing stability.

KB mirrors eliminate some of the shortcoming of the X-ray focusing lenses. They provide achromatic focusing and also act a harmonic rejection mirrors by not reflecting X-rays above a cutoff energy. For the CXI KB mirrors, the cutoff energy will be 11 keV with an incidence angle of 3.4 mrad and a SiC coating. The 1 micron KB mirror system is expected to produce a focus of roughly 1.3 μm depending on the photon energy as shown on Figure 4**.**

5.4.11. 0.1 micron KB mirrors. The requirements for the 0.1 micron KB mirror system are nearly identical to those of the 1 micron KB mirror system since both systems are diffraction limited. The only difference between the two systems is that the 0.1 micron mirrors have a curvature 10 times larger, with an average focal length of 0.7 m. The 1 micron KB mirrors will be retracted out of the beam to use the 0.1 micron KB mirrors and vice versa. The beam profiles as a function of photon energy calculated for perfect optics with finite apertures as shown on Figure 4 for both KB systems.

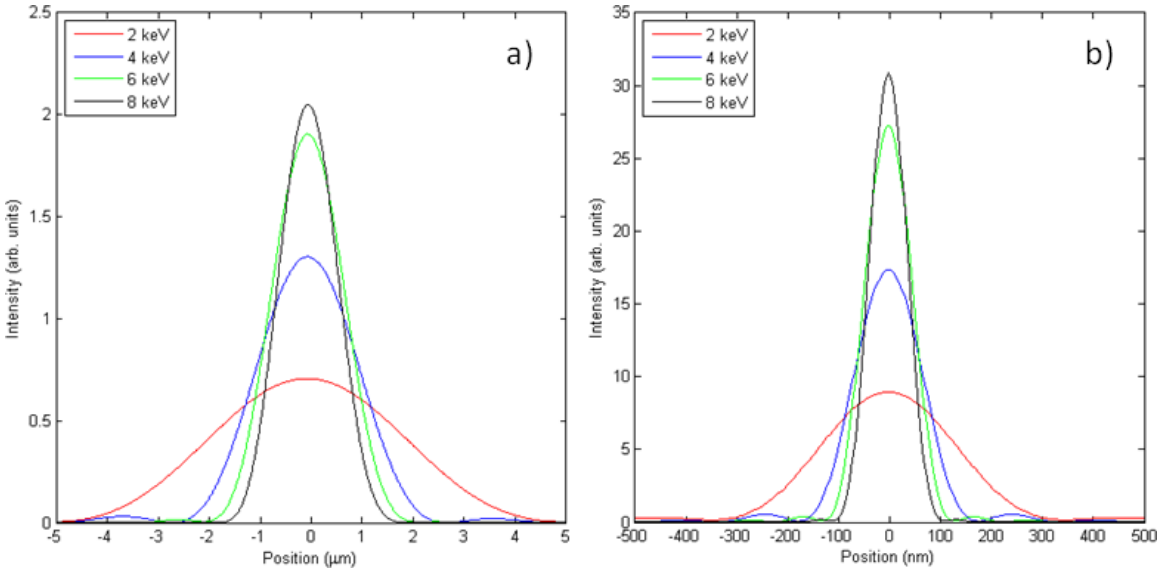

Figure 4: One dimensional beam profile at the focus of perfect CXI KB mirrors with finite apertures as a function of photon energy. The incident beam gets larger for lower energy which results in a larger focal spot. a) Profiles for the 1 micron KB mirrors. b) Profiles for the 0.1 micron KB mirrors. The profile shown was calculated for the downstream mirror of the 0.1 micron KB system which has a focal length of 0.5 m. The upstream mirror has a focal length of 0.9 m and will produce a larger spot size.

5.4.12. 0.1 micron sample chamber. The 0.1 micron sample chamber will be used exclusively with the 0.1 micron KB mirrors. The chamber will provide a high vacuum environment in which samples will be either held and positioned using stages or the samples will be delivered as a particle beam to the interaction region. The 0.1 micron sample chamber also provides an interface for the particle injector. Additionally, it contains multiple apertures to clean up the halo around the central beam and reduce the noise level on the detector. The main requirements of the 0.1 micron sample chamber are:

- accommodate multiple experiments configurations (fixed targets, injected particles);
- interface with the area detector downstream, the particle injector and the ion time-of-flight(TOF) spectrometer;
- provide ports for the introduction of pump lasers;
- vacuum of 10^{-7} torr;
- rapid access when venting is required;
- large volume for flexibility;
- on-axis sample viewing.

The 0.1 micron sample chamber will only be used with the beam focused by the 0.1 micron KB mirror system.

5.4.13. 1 micron sample chamber. The requirements of the 1 micron sample chamber are identical to those of the 0.1 micron sample chamber except that for the fact that the 1 micron sample chamber can be used with the direct unfocused LCLS beam, the 10 μm focus beam produced by the X-ray focusing lenses located 60 m away in the X-Ray Tunnel and the 1 μm focus beam produced by the 1 micron KB mirrors. The design of both sample chambers follows the same concepts as previously used for experiments at FLASH[14].

5.4.14. 120 Hz area detector. A very unique detector is required for CXI in order to measure the 2D coherent diffraction patterns from the sub-micron samples. The requirements for this detector are:

- <1 photon readout noise;
- 110x110 μm^2 pixel size;
- minimum 1500x1500 pixels;
- minimum 10^3 dynamic range;
- 120 Hz readout; and
- tiled modules with a variable hole size.

The low noise is required in order to be able to confidently distinguish between zero and one photon arriving at a pixel for weakly scattering samples. For single-molecule imaging experiments, recently proposed algorithms have been shown to work with as little as 0.04 photons/pixel on average at the highest resolution[29]. This is roughly the signal level expected for single-molecule experiments at CXI. Therefore, at the highest resolution, counts of one or zero photons are expected and it is required to distinguish them reliably.

The 120 Hz readout is required to fully utilize the capabilities of LCLS by reading out the data for every pulse. A 10^3 dynamic range is suitable for CXI experiments, especially if the hole in the middle of the detector can be varied and made large enough so that a second detector behind can be used to fill in the missing data. The CXI detector will have a variable hole size from 1 to 9.5 mm) which can be changed without removing the detector from vacuum. In order to build such a detector with a high dynamic range and low noise, a sacrifice must be made by having large pixels of 110 μm. For most CXI experiments, the only implication of the larger pixels is that the detector has to be moved farther away, which is easily accomplished.

5.4.15. Detector stage. The CXI detector will be mounted in vacuum inside the CXI detector stage. This stage serves the purpose of positioning the detector relative to the sample and the incoming beam. It will center the detector hole on the LCLS direct beam to prevent damage to the detector and it also will position the detector at the appropriate distance from the interaction region. The requirements are:

- range along the beam of 50-2400 mm,
- vacuum better than 10^{-7} torr,
- diagnostics behind the detector for alignment,
- transverse positioning accuracy better than 1 pixel, and
- stability better than 1 pixel.

The detector stage will have a continuous positioning range of 500 mm along the beam in vacuum and the entire system can be positioned at various mounting locations to cover the full range of positions. With the range of sample to detector distance available, the CXI instrument will allow objects as large as 3 μm to be oversampled by a factor of 2 using the 4 keV x-rays and as large as 1.5 μm using the 9 keV x-rays. The maximum object which can be imaged is given by $D=\lambda L/sd$ where L is the sample to detector distance, s is the oversampling ratio and d is the pixel size of 110 μm. Any object smaller than 1.5 μm can be oversampled by at least a factor of 2 and more if a longer wavelength is used. A minimum oversampling of 2 is required in order for phase retrieval techniques to be successful.

The resolution achievable is given by $\delta=2\lambda D/Nd$ where N is the number of pixels in 1 direction. Therefore the resolution which can be achieved with this detector is $\delta=2sD/N$ and with an oversampling ratio of 2 and N=1500 gives $\delta=D/375$. This means the experimental geometry will

allow at best an object to be imaged with 375 resolution elements. For example, a 375 nm object could be imaged with 1 nm resolution.

There is a fundamental limit to the resolution from the bandwidth of the LCLS as described in [48]. This limit is essentially 2500 resolution elements based on the temporal coherence of the LCLS. This indicates that a detector with more pixels would be a valuable addition to the CXI instrument in order to reach fundamental limit of LCLS.

5.4.16. Particle injector. The CXI particle injector will be based on developments at FLASH and will use aerodynamic lens technology to transfer an aerosol from atmospheric pressure into the high vacuum of the sample chamber and deliver free-standing samples to the LCLS beam[16, 17]. The particle injector can be mounted on either sample chamber, depending on which one is used for a given experiment. The requirements for the particle injector are:

- < 250 microns particle beam focus,
- > 50 % transmission,
- 10 mm steering range,
- 10 – 1000 nm particle size range, and
- particle beam diagnostics such as charge detectors[49].

The particle injector will be compatible with any type of samples whether they are organic, inorganic, amorphous or crystalline. Also, the positioning stage of the particle injector will be compatible with any other type of sample delivery system as long as it interfaces to a 6 inch Conflat flange. The system is versatile and allows integration of user-supplied sample delivery systems.

5.4.17. Ion Time-of-Flight. The purpose of the Ion Time-of-Flight is to detect ions produced by an exploding sample after its interaction with the LCLS beam. The measured spectra from the ITOF will provide at the very least a non-equivocal, “veto” trigger signal indicating that a particle was hit by the beam. Such a veto is required due to the random arrival of particles in the interaction region and the a priori uncertainty about whether a given pulse will hit any injected particle. The ITOF will also provide the ability to identify impurities and unwanted particles that were hit by the beam. The ITOF will allow the mass to charge ratio of the ions to be determined and the presence of some unwanted ionic species will allow rejection of the data as an unwanted sample. The requirements are:

- 1 Atomic Mass Unit resolution,
- up to 100 AMU detection,
- 1 GHz digitization, and
- does not interfere with imaging detector.

The last requirement highlights that the primary purpose of the CXI instrument is imaging and not detecting ions. In order to obtain high resolution from a TOF, one usually requires electrodes located close to the interaction region. These electrodes will often interfere with components needed for imaging, for example, apertures or the 2D detector. In such a case, the performance of the ITOF is sacrificed at the benefit of a better performing imaging system.

5.5. Conceptual design and layout

The conceptual layout of the CXI instrument is shown in Figure 5. Some components whose function does not require proximity to the sample will be placed in the X-Ray Tunnel. These devices are the attenuators, the pulse picker, slits and an intensity-position monitor which allows

non-destructive beam intensity measurement. The in-line x-ray focusing lenses are also located in the XRT. All of these devices are shared with the XCS instrument located in Hutch 4. The beam will then traverse all of Hutch 4 untouched before arriving in Hutch 5. The reference laser will be installed at the very beginning of Hutch 5 and will be used to align all of the downstream components. More slits will be used to clean up the beam and diagnostics will allow the quality of the beam and the effect of the upstream optics to be measured.

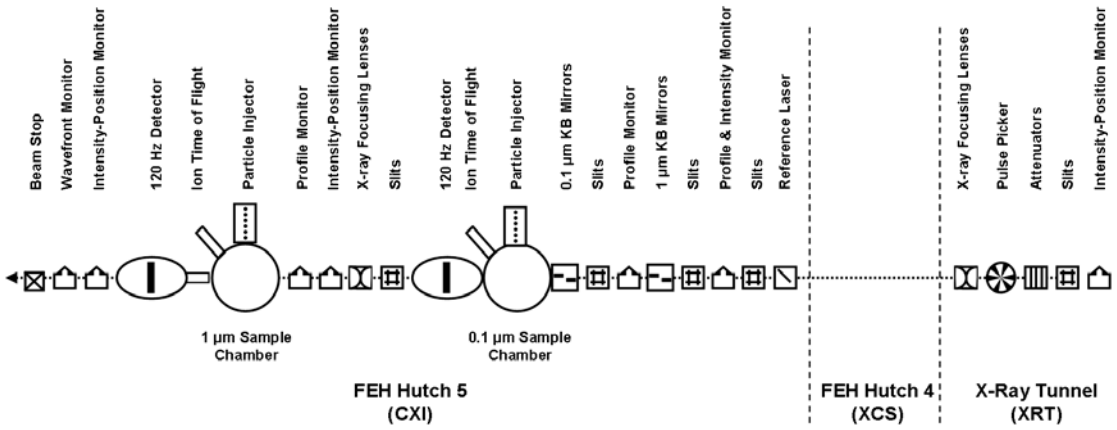

Figure 5: Conceptual layout of the Coherent X-ray Imaging (CXI) instrument at the Linac Coherent Light Source (LCLS). The beam travels from right to left. Some CXI devices are installed in the X-Ray Tunnel and the beam passes through Hutch 4 of the Far Experimental Hall (FEH) where the X-ray Correlation Spectroscopy (XCS) instrument is located. The majority of the CXI components are installed in Hutch 5 of the FEH.

5.5.1. Unfocused beam. If the users choose to use the unfocused LCLS beam, which will be roughly 1 mm wide at the CXI instrument, all focusing optics can be retracted, the 1 micron sample chamber will be aligned to the direct beam and only the slits and all diagnostics will be used along with the 1 micron sample chamber and the detector.

5.5.2. 10 micron focus. The 10 micron focal plane will be located in the 1 micron sample chamber and obtained by inserting the x-ray focusing lenses located in the XRT. The beam will be on the same axis as the unfocused beam requiring the same alignment of the system. The diagnostics in Hutch 5 will be unusable without attenuation of the beam in this mode since it will already be small by the time it reaches the hutch and will cause the diagnostics to be damaged. It will also not be possible to close the slits into the main beam since they will also degrade in the focused beam. The minimum slit opening in the hutch will be at least 500 µm in this mode. All focusing optics inside the hutch will be removed from the beam path. The beam at the wavefront monitor will unfortunately be too small (~100 microns) to make that device useful for anything other than measuring the low angle, missing data that passes through the center of the 2D CXI detector.

5.5.3. 1 micron focus. The 1 micron KB mirrors will be inserted in the beam and produce a focus at the center of the 1 micron sample chamber. Diagnostics downstream of the 1 micron KB mirrors will be used to align the mirrors and slits will be used to clean up the beam before and after the mirrors. All other focusing optics will be removed from the beam path. The intensity-

position monitor after the mirrors will be used to measure the incoming intensity non-destructively. The 1 micron sample chamber will be rotated to align with the new beam direction after the deflection by the 1 micron KB mirrors and the CXI detector will be used in combination with the diagnostics at the downstream end of the hutch. The wavefront monitor will be located 8 m downstream of the focus so that the beam at this plane will be roughly the same size as the unfocused beam, or about 1 mm. This will allow direct imaging of the beam intensity downstream of the focus. The intensity-position monitor at the back of the hutch can also provide a redundant intensity measurement for normalization.

5.5.4. 0.1 micron focus. If the users wish to use the 0.1 μm focus, the 1 micron KB mirrors and both X-ray focusing lenses will be retracted and the 0.1 micron KB mirrors will be inserted in the beam path. This will produce a 0.1 μm FWHM spot in the 0.1 micron sample chamber, some 0.7 m downstream of the mid point between the mirrors. The sample will be supported or delivered using the particle injector into the 0.1 micron sample chamber on which the CXI detector will be attached. The short focal length of these mirrors will cause a highly divergent beam to grow to 1 mm in size 0.7 m downstream of the focal plane. Therefore, the profile monitor installed before the 1 micron Sample Chamber can be used as a second detector to measure the low angle signal passing through the hole in the main detector. The profile monitor can also be used as a wavefront monitor and the beam would terminate there in this case. The 1 micron sample chamber would not be used in this case.

5.5.5. Refocus into the 1 micron Sample Chamber. A second set of X-ray focusing lenses will be installed inside Hutch 5 between the two sample chambers. When the beam is focused into the 0.1 micron sample chamber by the 0.1 micron KB mirrors, it can be refocused using the X-ray focusing lenses and a second experiment can be run in series inside the 1 micron sample chamber. This will allow, in cases where the primary experiment in the upstream sample chamber does not require any diagnostics downstream of the focus, to run a parasitic experiment by reusing the beam again in the downstream sample chamber.

5.5.6. Experiments at atmospheric pressure. The CXI instrument is designed to run completely in vacuum. However, it will be possible to run experiments at atmospheric pressure in both sample chambers. For the 0.1 micron sample chamber, a diamond window will separate the 0.1 micron KB mirrors vacuum tank from the sample area allowing experiments to be performed in air. The close proximity of the mirrors to the focus in this case requires the mirror and sample-vacuum tanks to be integrated and it will not be possible to remove the 0.1 micron sample chamber. Experiments using the 0.1 micron focus will always be performed inside the 0.1 micron sample chamber, whether they are conducted under vacuum or at atmospheric pressure.

For the 1 micron sample chamber, another diamond window can be inserted upstream of the chamber allowing experiments to be performed in poor vacuum or at atmosphere. It will also be possible to completely remove the 1 micron sample chamber and install a completely separate system for experiments that can be performed in air.

5.6. Possible upgrades

5.6.1. Monochromator. The CXI instrument in its initial version will not have a monochromator since the majority of experiments envisioned for CXI require the full beam intensity and do not suffer from the 0.2% bandwidth of the beam. However, a monochromator could be added to the instrument easily. It could be installed in the XRT since space was reserved for CXI upgrades in that area.

5.6.2. Pump laser system. Dynamic processes induced by a pump laser pulse could be imaged with the addition of a pump laser system for CXI. These types of pump-probe imaging experiments are expected to become an important part of the CXI science program once a laser system is available. A laser could be added inside the CXI hutch directly or located in an adjacent room to the CXI instrument and sent to the experiment inside an evacuated beam pipe.

5.6.3. Cryo-stage. The initial version of the CXI instrument will provide two methods to introduce samples in the beam: a room temperature fixed target system and a particle injector based on aerosol techniques and aerodynamic lenses. The first method is most often not suitable for biological samples, which will dehydrate and denature if transferred to vacuum this way. The second method requires a large number of samples since the sample arrival at the interaction region is random and therefore only a small fraction of the samples delivered will be hit by the LCLS beam. The technique is not suitable for rare samples of which only a few thousands or fewer copies exist. If those rare samples are also biological, then they cannot be mounted on the room temperature fixed target stage. A cryo-stage similar to those used in cryo electron microscopy would be extremely useful to flash freeze these rare samples and then transfer them to vacuum in a frozen-hydrated state. The CXI instrument team is currently investigating possibilities to add such a cryo-stage to the system.

6. Summary

Table 2: Summary of key CXI parameters.

Parameters	**10 micron focus**	**1 micron focus**	**100 nm focus**	**Units**
Focusing optic	Be lenses	KB	KB	
Low photon energy cutoff	~ 4	~ 2	~ 2	keV
High photon energy cutoff	25	11	11	keV
Spot size (FWHM V x H)	10 x 10	1.3 x 1.3	0.090 x 0.150	μm^2
Divergence	140	12	1.4	mrad
Power density	$3x10^{16}$	$3x10^{18}$	$3x10^{20}$	W/cm^2
Photon bandwidth	~0.2	~0.2	~0.2	%
Rayleigh length (at 9 keV)	100 mm	1.6 mm	8 (V) x 21 (H) µm	

In summary, the Coherent X-ray Imaging instrument has been designed to be flexible and provide users with many options to perform unique imaging experiments using the LCLS beam. The

instrument will provide a versatile focusing system and a suite of shot-to-shot diagnostics, as well as optics to tailor the beam properties to the user needs. A summary of the key CXI beam parameters is given in Table 2. The CXI instrument will also provide two independent sample environments capable of performing fixed-target measurements. The sample environments will also interface with a free-standing sample delivery system that will be part of the CXI-supplied suite of equipment. A custom-made detector capable of reading out full 2D images at 120 Hz, the maximum repetition rate of LCLS, will be available to users for experiments. The instrument is now in the construction phase and user operations will begin in 2011.

7. Acknowledgements

The authors wish to acknowledge members of the LCLS and LUSI project scientific staff who helped develop the requirements for the devices described. Specifically, the authors wish to thank Yiping Feng, David Fritz, Jerry Hastings, Marc Messerschmidt, Aymeric Robert and Niels van Bakel. The authors also owe special gratitude to Paul A. Montanez for the help in fine-tuning te conceptual design reconciling desires with real-world feasibility. Finally special thanks are owed to the CXI team leaders, Henry Chapman, Janos Hajdu and John Miao, who were instrumental in getting this project started. The work presented has been funded by the LCLS Ultrafast Science Instruments (LUSI) project. The Linac Coherent Light Source is a national user facility operated by Stanford University on behalf of the U.S. Department of Energy, Office of Basic Energy Sciences.

1. Fienup, J R, 1982. *Applied Optics*. **21**(15): p. 2758-2769.
2. Marchesini, S, He, H, Chapman, H N, Hau-Riege, S P, Noy, A, Howells, M R, Weierstall, U and Spence, J C H, 2003. *Physical Review B*. **68**(14): p. 140101.
3. Marchesini, S, 2007. *Journal of the Optical Society of America a-Optics Image Science and Vision*. **24**(10): p. 3289-3296.
4. Sayre, D, Chapman, H N and Miao, J, 1998. *Acta Crystallographica Section A*. **54**: p. 232-239.
5. Miao, J W, Charalambous, P, Kirz, J and Sayre, D, 1999. *Nature*. **400**(6742): p. 342-344.
6. Pfeifer, M A, Williams, G J, Vartanyants, I A, Harder, R and Robinson, I K, 2006. *Nature*. **442**(7098): p. 63-66.
7. Abbey, B, Nugent, K A, Williams, G J, Clark, J N, Peele, A G, Pfeifer, M A, De Jonge, M and McNulty, I, 2008. *Nature Physics*. **4**(5): p. 394-398.
8. Thibault, P, Dierolf, M, Menzel, A, Bunk, O, David, C and Pfeiffer, F, 2008. *Science*. **321**(5887): p. 379-382.
9. Williams, G J, Quiney, H M, Peele, A G and Nugent, K A, 2007. *Physical Review B*. **75**(10): p. 104102.

10. Howells, M R, *et al.*, 2009. *Journal of Electron Spectroscopy and Related Phenomena*. **170**(1-3): p. 4-12.
11. Neutze, R, Wouts, R, van der Spoel, D, Weckert, E and Hajdu, J, 2000. *Nature*. **406**(6797): p. 752-757.
12. Saldin, E L, Schneidmiller, E A and Yurkov, M V, 1995. *Physics Reports-Review Section of Physics Letters*. **260**(4-5): p. 187-327.
13. Ayvazyan, V, *et al.*, 2006. *European Physical Journal D*. **37**(2): p. 297-303.
14. Chapman, H N, *et al.*, 2006. *Nature Physics*. **2**(12): p. 839-843.
15. Boutet, S, Bogan, M J, Barty, A, Frank, M, Benner, W H, Marchesini, S, Seibert, M M, Hajdu, J and Chapman, H N, 2008. *Journal of Electron Spectroscopy and Related Phenomena*. **166**: p. 65-73.
16. Bogan, M J, *et al.*, 2008. *Nano Letters*. **8**(1): p. 310-316.
17. Bogan, M J, *et al.*, 2010. *Aerosol Science and Technology*. **4**(3): p. i-vi.
18. Ding, Y, *et al.*, 2009. *Physical Review Letters*. **102**(25): p. 254801.
19. Bane, K L F, *et al.*, 2009. *Physical Review Special Topics-Accelerators and Beams*. **12**(3): p. 030704.
20. Akre, R, *et al.*, 2008. *Physical Review Special Topics-Accelerators and Beams*. **11**(3): p. 030703.
21. Barty, A, Soufli, R, McCarville, T, Baker, S L, Pivovaroff, M J, Stefan, P and Bionta, R, 2009. *Optics Express*. **17**(18): p. 15508-15519.
22. Schmidt, K E, Spence, J C H, Weierstall, U, Kirian, R, Wang, X, Starodub, D, Chapman, H N, Howells, M R and Doak, R B, 2008. *Physical Review Letters*. **101**(11): p. 115507.
23. DePonte, D P, Weierstall, U, Schmidt, K, Warner, J, Starodub, D, Spence, J C H and Doak, R B, 2008. *Journal of Physics D-Applied Physics*. **41**(19): p. 195505.
24. DePonte, D P, Doak, R B, Hunter, M, Liu, Z Q, Weierstall, U and Spence, J C H, 2009. *Micron*. **40**(4): p. 507-509.
25. Weierstall, U, *et al.*, 2008. *Experiments in Fluids*. **44**(5): p. 675-689.
26. Chapman, H N, *et al.*, 2006. *Journal of the Optical Society of America a-Optics Image Science and Vision*. **23**(5): p. 1179-1200.
27. Bortel, G, Faigel, G and Tegze, M, 2009. *Journal of Structural Biology*. **166**(2): p. 226-233.
28. Bortel, G and Faigel, G, 2007. *Journal of Structural Biology*. **158**(1): p. 10-18.
29. Fung, R, Shneerson, V, Saldin, D K and Ourmazd, A, 2009. *Nature Physics*. **5**(1): p. 64-67.
30. Loh, N T D and Elser, V, 2009. *Physical Review E*. **80**(2): p. 026705.
31. Huldt, G, Szoke, A and Hajdu, J, 2003. *Journal of Structural Biology*. **144**(1-2): p. 219-227.
32. Eisebitt, S, Luning, J, Schlotter, W F, Lorgen, M, Hellwig, O, Eberhardt, W and Stohr, J, 2004. *Nature*. **432**(7019): p. 885-888.
33. Schlotter, W F, *et al.*, 2007. *Optics Letters*. **32**(21): p. 3110-3112.
34. Schlotter, W F, *et al.*, 2006. *Applied Physics Letters*. **89**(16): p. 214410.
35. Shintake, T, 2008. *Physical Review E*. **78**(4): p. 041906.
36. Marchesini, S, *et al.*, 2008. *Nature Photonics*. **2**(9): p. 560-563.
37. Williams, G J, Quiney, H M, Dahl, B B, Tran, C Q, Peele, A G, Nugent, K A, De Jonge, M D and Paterson, D, 2007. *Thin Solid Films*. **515**(14): p. 5553-5556.

38. Kang, H C, *et al.*, 2008. *Applied Physics Letters*. **92**(22): p. 221114.
39. Boutet, S and Robinson, I K, 2006. *J Synchrotron Radiat*. **13**(Pt 1): p. 1-7.
40. Boutet, S and Robinson, I K, 2007. *Physical Review E*. **75**(2): p. 021913.
41. Boutet, S and Robinson, I K, 2008. *Journal of Synchrotron Radiation*. **15**: p. 576-583.
42. Barty, A, *et al.*, 2008. *Nature Photonics*. **2**(7): p. 415-419.
43. Alexander, A J and Camp, P J, 2009. *Crystal Growth & Design*. **9**(2): p. 958-963.
44. Vartanyants, I A, Robinson, I K, McNulty, I, David, C, Wochner, P and Tschentscher, T, 2007. *Journal of Synchrotron Radiation*. **14**: p. 453-470.
45. Narayanan, R, Tabor, C and El-Sayed, M A, 2008. *Topics in Catalysis*. **48**(1-4): p. 60-74.
46. Le Bolloc'h, D, Livet, F, Bley, F, Schulli, T, Veron, M and Metzger, T H, 2002. *Journal of Synchrotron Radiation*. **9**: p. 258-265.
47. Lengeler, B, Schroer, C G, Kuhlmann, M, Benner, B, Guenzler, T F, Kurapova, O, Zontone, F, Snigirev, A and Snigireva, I, 2005. *Journal of Physics D-Applied Physics*. **38**(10A): p. A218-A222.
48. Hau-Riege, S P, 2008. *Optics Express*. **16**(4): p. 2840-2844.
49. Benner, W H, Bogan, M J, Rohner, U, Boutet, S, Woods, B and Frank, M, 2008. *Journal of Aerosol Science*. **39**(11): p. 917-928.